ARTICLE IN PRESS

Ain Shams Engineering Journal xxx (xxxx) xxx

Contents lists available at ScienceDirect

Ain Shams Engineering Journal

journal homepage: www.sciencedirect.com

Artificial intelligence approach in mixed convection heat transfer under transverse mechanical vibrations in a rectangular cavity

Somayeh Davoodabadi Farahani [a,*], As'ad Alizadeh [b], Mohammed A. Tashkandi [c], Lioua Kolsi [d], Aliakbar Karimipour [e,f,*]

[a] School of Mechanical Engineering, Arak University of Technology, 38181-41167, Arak, Iran
[b] Department of Civil Engineering, College of Engineering, Cihan University-Erbil, Erbil, Iraq
[c] Mechanical Engineering Department, College of Engineering, Northern Border University, Arar, Saudi Arabia
[d] Department of Mechanical Engineering, College of Engineering, University of Ha'il, Ha'il City 81451, Saudi Arabia
[e] Institute of Research and Development, Duy Tan University, Da Nang, Vietnam
[f] School of Engineering & Technology, Duy Tan University, Da Nang, Vietnam

ARTICLE INFO

Keywords:
Mixed convection heat transfer
Sinusoidal oscillations
Mechanical vibrations
Artificial intelligence GMDH

ABSTRACT

In the current research, the mixed convection heat transfer in a rectangular chamber with walls with sinusoidal oscillations and mechanical vibrations has been investigated. Mechanical vibrations on the chamber, sinusoidal oscillations of the hot wall and flow due to buoyancy are considered. The finite volume method is utilized for simulation. The efficacy of changes in governing parameters, such as frequency, oscillation amplitude, *Ra*, chamber length to width ratio, change of fluid type on *Nu* has been investigated. The results indicate that there is an optimal ratio of chamber dimensions that has the maximum *Nu* in the fixed *Ra*, and this ratio depends on the type of fluid. In the presence of sinusoidal oscillations of the hot wall and transverse mechanical vibrations of the cylinder, it increases the heat transfer by about 96 % and 75 %, respectively, compared to the state without vibration. The increase in the frequency and amplitude of oscillations in the case where the hot wall oscillates sinusoidally is negligible on the Nusselt number. Increasing the frequency and amplitude of oscillations of transverse vibrations of the chamber has a significant efficacy on *Nu*, and the amplitude of oscillations has a greater efficacy than the frequency of oscillations on heat transfer. Based on the available data and using artificial intelligence, GMDH, *Nu* has been estimated. The results indicate that this modeling has been able to estimate the Nusselt number with good accuracy with $R^2 = 0.948$.

1. Introduction

Free convection is one of the popular methods of heat transfer (HT) that has been the attention of researchers for a long time, and numerous studies have been directed on it. Among these, free convection(FC) in a cavity can be considered as one of the simplest geometries related to free convection that has been extensively studied [1–3]. For instance, Nakamura et al. [4] has conducted a study in this field, examining the effect of temperature differences in creating immersion movements in the fluid. Sharif et al. [5]studied a rectangular chamber with an upper wall moving at a constant speed. They also continued to analysis the result of different aspect ratios of the chamber on combined convection.

Using the finite element method, Saberi et al. [6] simulated the interaction of fluid and structure inside a parallelogram chamber with an elastic vane in the middle to investigate FC-HT. In their study, the right wall was completely in cold temperature, while only one third of the left wall of the chamber was in hot temperature, and the other boundaries were considered as insulation. By examining the parameters of the ratio of conductivity coefficient and Young's modulus of the elastic vane, they exhibited that increasing the ratio of conductivity coefficient increases HT, and the stiffness of Young's modulus helps to improve convective heat transfer. Saleh et al. [7], considering the interaction effects between fluid and solid, investigated natural convection heat transfer inside a closed chamber comprising two flexible vanes and a constant temperature heat source. The heat source was in the center of the chamber and the fins were vertically connected to the upper wall of the chamber. Their results specified that very small fluctuations of the flexible blade have a significant efficacy on the HT, average *Nu*, flow line patterns and temperature. Also, increasing the

* Corresponding authors at: Institute of Research and Technology, Duy Tan University, Da Nang, Vietnam (A. Karimipour).
E-mail addresses: sdfarahani@arakut.ac.ir (S. Davoodabadi Farahani), aliakbarkarimipour@duytan.edu.vn (A. Karimipour).

https://doi.org/10.1016/j.asej.2024.103012
Received 19 May 2024; Received in revised form 25 July 2024; Accepted 3 August 2024

Please cite this article as: Somayeh Davoodabadi Farahani et al., *Ain Shams Engineering Journal*, https://doi.org/10.1016/j.asej.2024.103012

Nomenclature

C_p	specific heat capacity ($J.kg^{-1}.K^{-1}$)
A	Amplitude(mm)
f	Frequency(Hz)
g	Gravitational acceleration ($m.s^{-2}$)
Gr	Grashof number
H	height (m)
k	Thermal conductivity ($W.m^{-1}.K^{-1}$)
L	length (m)
Nu	Nusselt number
P	Pressure (Pa)
q"	Heat flux ($W.m^{-2}$)
R^2	absolute fraction of variance
Ra	Rayleigh number
T	temperature (K)
t	Time (s)
u, v	Velocity component in x- and y direction ($m.s^{-1}$)
x,y	Cartesian coordinate

Subscripts

f	Fluid
H	High
L	Low
nf	Hybrid nanofluid
O	Ambient

Greek letter

β	Thermal expansion coefficient (K^{-1})
μ	Dynamic viscosity (Pa.s)
ν	Kinematic viscosity ($m^2.s^{-1}$)
ρ	Density ($kg.m^{-3}$)
α	Thermal diffusion coefficient($m^2.s^{-1}$)
φ	Volume fraction
ω	Frequency of mechanical vibration (Hz)

Abbreviations

AI	Artificial intelligence
ANN	artificial neural network
BC	boundary conditions
FC	free convection
FVM	Finite volume method
GMDH	Group Method of Data Handling
HT	Heat transfer
NF	Nanofluid
NN	Neural network
NPs	Nanoparticles
RMSE	root mean square error
SVM	Support vector machine
UDF	User Defined Function

length and amplitude of blade oscillations reduces the HT on the cold wall and increases *Nu* on the hot source. Kim et al. [8]inspected the efficacy of a circular heat source on the *Nu* inside square chambers with cold walls. They acknowledged the average *Nu* for several values of *Ra* from 0 to 4, that at low values of *Ra*, four weak symmetric vortices around the heat source and at high values of *Ra*, two strong vortices are formed around the heat source. Surtiji et al. [9] inspected the effect of various parameters such as volume fraction of nanofluid, *Ra*, heat source radius on *Nu* in a chamber with a triangular cross-section filled with water-copper nanofluid containing an internal heat source. Their outcomes disclosed that with the increase of the radius of the heat source, the value of the average *Nu* increases in very large values of the *Ra* and decreases in the low values of the *Ra*. They also showed that the addition of NPs to the base fluid increases the HT inside the chamber, and the percentage of this increase was more significant at low *Ra*. Al Qahtani et al. [10] inspected the combination of entropy production and convection in a chamber with five barriers under a uniform magnetic field, along with volume radiation for solar collectors. The simulation results indicated that the presence of radiation waves decreased the total entropy produced, resulting in maximum entropy production when radiation was absent. Buanani et al. [11] investigated the combined impacts of natural convection and volume radiation in a concentric square ring. The findings revealed that radiation had a notable influence on the current and temperature distribution for *Ra* based on the Planck number. In other studies, the effect of nanofluid [12–15] and magnetic field [16,17] on mixed convection heat transfer has been investigated. The porous medium [18–21] can also help to improve convection heat transfer by changing the thermal conductivity coefficient.

Several studies [22–25] have explored vibrational convection, which holds significant potential for various requests. Florio and Harnoy [25] examined the utilization of a fluctuating plate to mend HT from an obstruction inside an internal flow. Another application [26] involves the vibrational displacement effect in space on HT, where mechanically induced pseudo-gravity may be more significant in the presence of a weak gravitational field. Sarhan et al. [27] conducted an experiment to analyze the impact of vertical sinusoidal vibrations and orientation (horizontal and inclined at angles of 30°, 45°, and 60°) on a smooth heat sink plate exposed to natural convection. The experiment involved varying vibration amplitudes from 1.5 to 7.5 mm and frequencies from 0 to 16 Hz under constant heat flow conditions. Controlled vibrations of the pins using a small actuator were implemented to reduce resistance in turbulent flows and enhance their role in HT. Results indicated that higher vibration frequencies led to increased HT rates, with the most significant enhancement observed in the horizontal position at 16 Hz.

Ji et al. [28] directed a numerical search into the enhancement of HT through vibration in an innovative flexible passage tube bundle heat exchanger(HE). In a different study, Ji et al. [29] scrutinized the vibration and HT features of a modified flexible tube bundle HE. They indicated that the tube bundle exhibited significantly higher amplitude in the z-direction compared to the y-direction, with frequency and amplitude increasing within the design range when tube rows were spaced apart. Fluid-induced vibration led to an 11.67 % increase in the *Nu*. Rasangika et al. [30] conducted numerical investigations on square and sine wave vibration parameters to interrupt the flow for enhancing convection HT in heat sinks.

Recent scientific studies have increasingly utilized artificial intelligence (AI) and machine learning techniques for estimating CHT [31–34]. Researchers have employed AI algorithms such as ANN, genetic algorithms, and SVM to predict HT coefficients, *Nu*, and other key parameters in CHT-processes. These AI-based approaches offer advantages such as improved accuracy, faster computation, and the ability to handle complex data sets. By training machine learning models on experimental or numerical data, researchers can develop predictive tools that can enhance our understanding of convective HT phenomena and optimize heat exchanger designs. The integration of AI and machine learning methods in heat transfer research holds great promise for advancing the field and developing more efficient thermal management systems.

Based on previous studies, a lot of research has been conducted on convective HT under various boundary conditions, boundary layer slip, and geometry changes. However, the efficacy of oscillatory wall deformation on convective heat transfer has not been investigated so far. Therefore, the present study focuses on numerically investigating the influence of transverse mechanical vibrations of the enclosure and si-

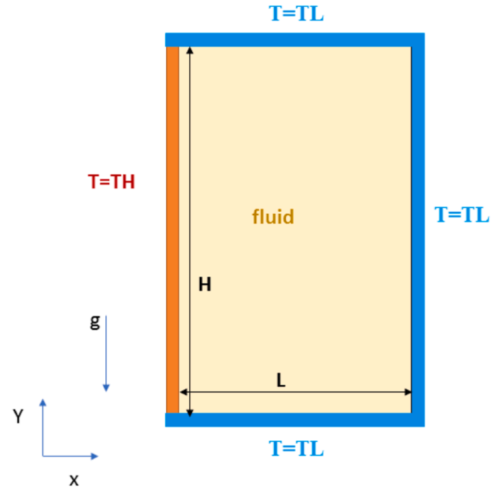

a)

	air	water	AL2O3
$C_p(\frac{J}{kgK})$	1006.4	4179	765
$\rho(\frac{kg}{m^3})$	1.22	997.1	3970
$k(\frac{W}{mK})$	0.0242	0.613	40
$\alpha(\frac{m^2}{s})$	7.44e-04	1.47e-06	131.7
$\beta(\frac{1}{K})$	0.00205	2.10e-05	-

b)

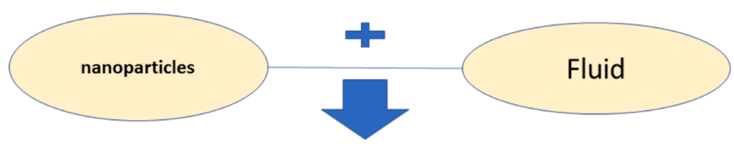

Nanofluid(nf)

$$\rho_{nf} = (1-\varphi)\rho_f + \varphi\rho_{np}$$

$$(\rho c_p)_{nf} = (1-\varphi)(\rho c_p)_f + \varphi(\rho c_p)_{np}$$

$$\mu_{nf} = \frac{\mu_f}{(1-\varphi)^{2.5}}$$

$$\frac{k_{nf}}{k_f} = \frac{k_{np} + (n-1)k_f - (n-1)\varphi(k_f - k_{np})}{k_{np} + (n-1)k_f + \varphi(k_f - k_{np})}$$

$$(\rho\beta)_{nf} = (1-\varphi)(\rho\beta)_f + \varphi(\rho\beta)_{np}$$

c)

Fig. 1. a) a schematic of case study, b)thermal features of materials[35], and c)Relationships to calculate nanofluid properties[36].

nusoidal wall oscillations on FC-HT. Using the finite volume method, the effect of the aspect ratio of the enclosure, *Ra*, sinusoidal wall oscillations, and transverse mechanical vibrations on convective HT from a rectangular enclosure has been examined. Additionally, artificial intelligence techniques have been used to estimate *Nu* in the enclosure based on available data. In the following, the structure of the paper is as follows: In the problem description section, the HT issue is elucidated, focusing on mathematical modeling, numerical solution, grid independence, validation, and modeling using artificial intelligence techniques. The discussion and results section extensively explores the efficacy of influential parameters on HT in the specified problem. Finally, based on the obtained data, artificial intelligence is employed to evaluation the *Nu*.

2. Description of the problem

2.1. Mathematical model and numerical solution

An illustration of the studied geometry and boundary conditions (BC's) are revealed in Fig. 1a. $T = T_H$ is employed on the left wall and $T = T_L$ is applied on the other walls and $T_H > T_L$. The $u = v = 0$ is applied on the walls. The thermophysical properties of the material are shown in Fig. 1b.

The height of the chamber is H and its width is L. In the state of the moving boundary, the left wall is transformed into a sine wave, and it is defined as follows [37]:

$$y(t) = \left(1 - A\sin(ft)\sin\left(\frac{2\pi x}{L}\right)\right) \quad (1)$$

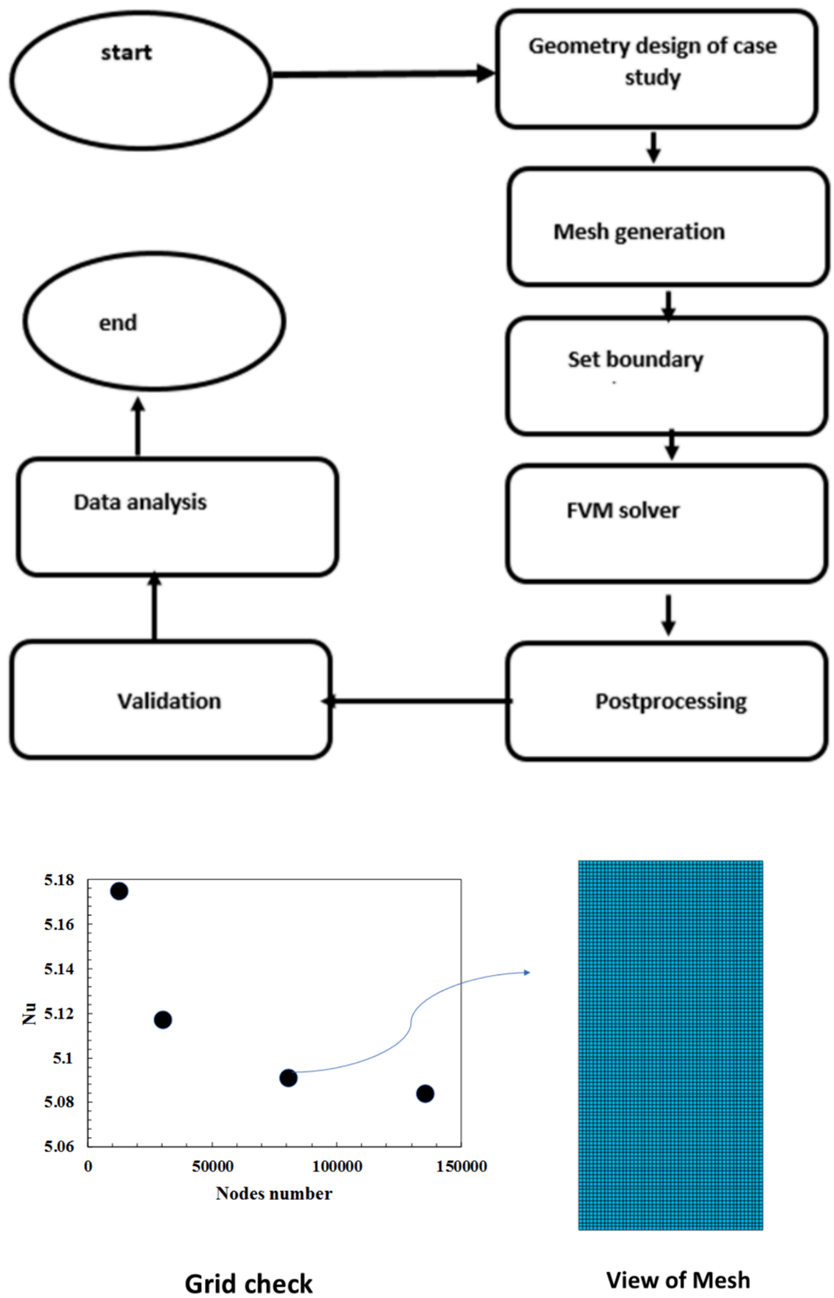

a)

b)

Fig. 2. a) flow chart of the planned technique, b) mesh study and view of the selected mesh, verification of the current study with the findings of c) Catton [42] and d) with previous studies[43–45].

where $y, A, f, t, x, andL$ are displacement, amplitude, frequency, time, x-direction, length of cavity, respectively. In the case that the enclosure is affected by mechanical vibrations, it vibrates in the y direction, and the vibration speed,$v_{0(t)}$, [38,39]is reported as follows:

$$v_{0(t)} = \omega H sin(\omega t) \tag{2}$$

Where t, and ω are the time and frequency of oscillation, respectively. Boussinesq approximation [40,41]is used for FC-HT. The governing equations for laminar flow and 2D are defined as follow as [14]:

$$\vec{\nabla}.\vec{V} = 0 \tag{3}$$

$$\left(\vec{\nabla}.\vec{V}\right).\vec{V} = -\frac{\vec{\nabla}(\mathrm{P})}{\rho} + \vartheta\nabla^2\vec{V} - (1 - \beta(T - T_o))\vec{g} + S_u \tag{4}$$

$$\vec{V}.\vec{\nabla}T = \alpha\nabla^2 T \tag{5}$$

The dimensionless numbers: Grashof (Gr), Rayleigh (Ra) and Nusselt (Nu), are stated as follows [20]:

$$\mathrm{Gr} = \frac{\mathrm{g}\beta(T_H - \mathrm{T_L})\mathrm{L}^3}{\left(\frac{\mu}{\rho}\right)^2} \tag{6}$$

c)

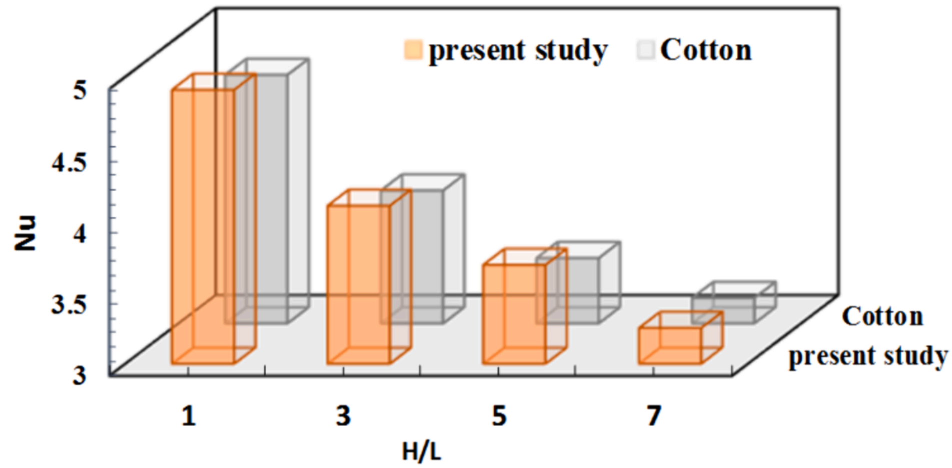

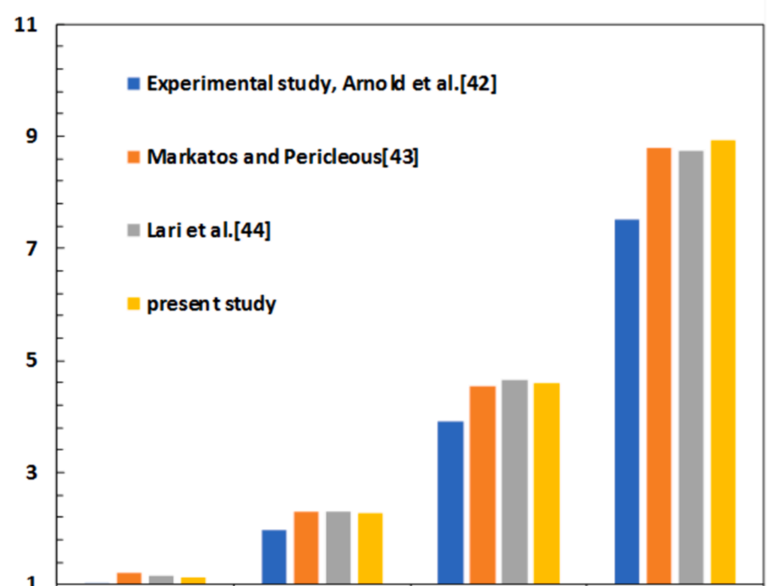

	Ra=1000	Ra=10000	Ra=100000	Ra=1000000
Experimental study, Arnold et al.[42]	1.008	1.973	3.913	7.505
Markatos and Pericleous[43]	1.208	2.301	4.53	8.804
Lari et al.[44]	1.161	2.3	4.646	8.752
present study	1.12	2.27	4.6	8.93

d)

Fig. 2. (*continued*).

$$\mathrm{Ra} = Gr\left(\frac{\mu}{\rho\alpha}\right) \quad (7)$$

$$\mathrm{Nu} = \frac{\mathrm{hL}}{\mathrm{k}} \quad (8)$$

Where ϑ,V, β, P, μ, k, ρ, h T, α and g characterize kinematic viscosity, velocity, thermal expansion coefficient, pressure, viscosity, thermal conductivity, density, convection HT coefficient, temperature, thermal diffusion coefficient and gravity acceleration, respectively. $S_u = Av_0(t)$ is momentum source terms in the mechanical vibration state. A is the amplitude of mechanical vibration. Relationships to calculate nanofluid properties [36] are displayed in Fig. 1c.

In this survey, Fluent ANSYS software is employed utilizing the FVM to solve the equations(3–5). The SIMPLE algorithm is employed to link P and V. The second-order upwind scheme is implemented for discretizing the equations, while the Presto scheme is employed for pressure correction. The relaxation coefficients for continuity, momentum, energy, and volume fraction equations are set at 0.3, 0.5, 1, and 0.9, respectively. Convergence bench mark for continuous, momentum and energy equations are 10^{-3}, 10^{-5} and 10^{-8}, respectively. Mechanical vibration is generated by S_u in the Y direction. The S_u in the Y direction is introduced into the fluid domain, controlled by a sine function definite in the UDF. When the left boundary undergoes sinusoidal changes, these variations are implemented using the UDF and dynamics mesh. The transient problem is solved in such scenarios, and after examining the impact of time step size on solution accuracy, a time step of 0.001 s has

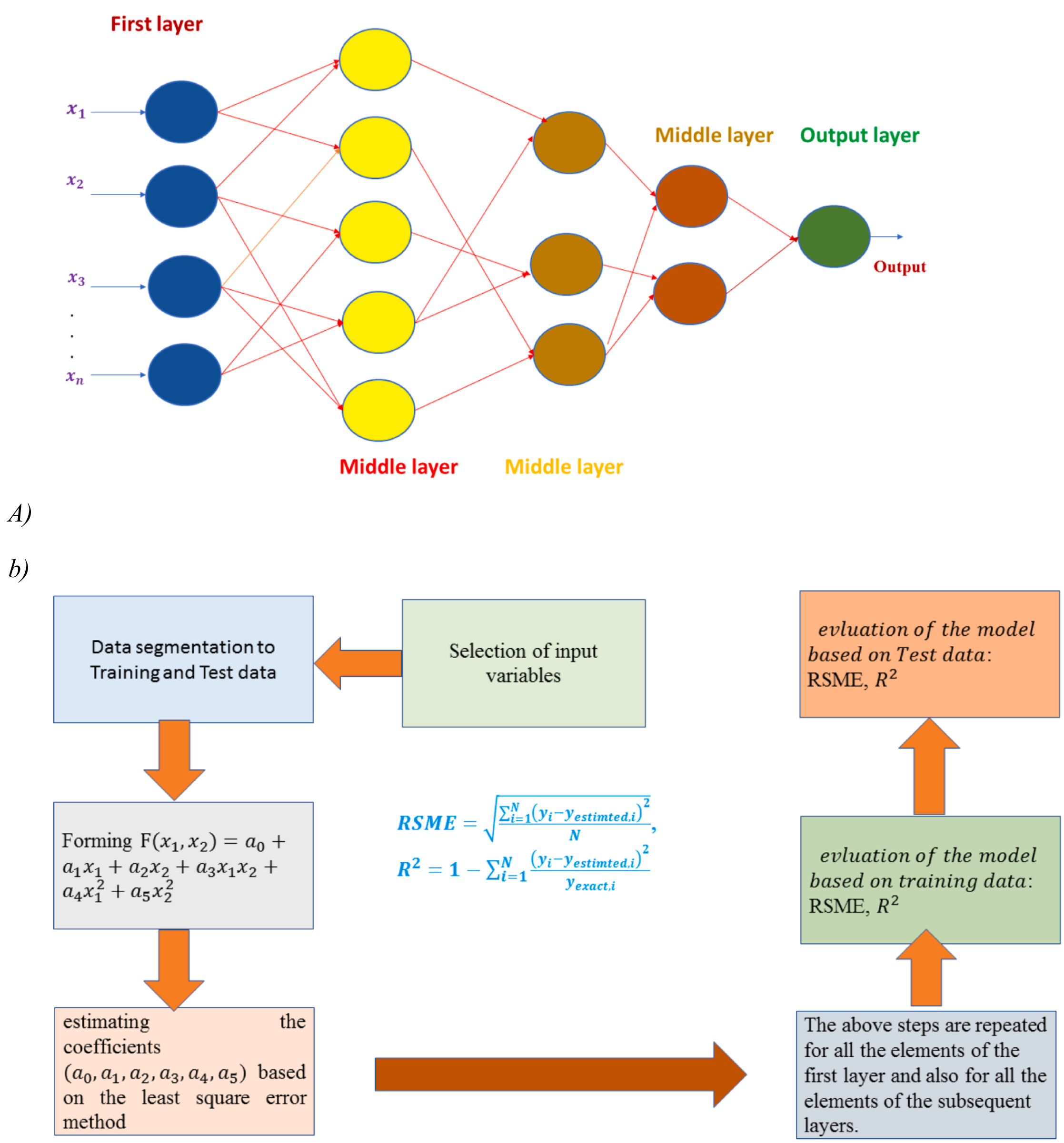

Fig. 3. a) schematic and b) algorithm of gmdh neural network structure[46,47].

been chosen for the simulations, with a final simulation time of 1 s. Flow chart of the proposed technique was illustrated in Fig. 2a.

The number of grid nodes meaningfully influences the accuracy and computational time of the numerical solution. The mesh consists of structured quadrilateral cells with varying spacing distributions. The resulting grid is locally orthogonal to the surface of the wall and is refined in areas where significant gradients are anticipated. Four grids with varying numbers of nodes were analyzed to study the variation in *Nu*. The findings of this investigation and a view of mesh are described in Fig. 2b. The findings specify that the solution accuracy improves as the grid size decreases. Consequently, the grid consisting of 80,601 nodes was chosen to proceed with the cavity calculations, as illustrated in Fig. 2b. The simulations are carried out on an Intel (R) Core i7 with a CPU6700K 4 GHz and 16 GB RAM. The solution time for various test modes ranges from 7322 to 8456 min.

The *Nu* in the cavity is compared to the findings of Catton [42] for Ra $= 10^5$ and the outcomes are presented in Fig. 2c. The comparison reveals a strong agreement between the existing modeling and the referenced work, with a maximum difference of less than 8 %. It is evident that as H/L increases at Ra $= 10^5$, the *Nu* declines. The widening gap among the plates limits fluid mixing by reducing the interaction between hot and cold fluids, leading to a decrement in the average fluid temperature. Also, in the following, *Nu* for $\frac{H}{L} = 1, T_H = 30^{\circ} C and T_L = 10^{\circ}C$ is compared with previous studies [43–45] and displayed in Fig. 2d. *Nu* calculated in our study align closely with Ref. [43–45]. The average deviation is below 15 %, confirming the accuracy of the current study.

2.2. GMDH algorithm-Neural network model

The Group Method of Data Handling [46,47], abbreviated as GMDH, is a linear regression and modeling method. The schematic and algorithm of the GMDH –NN structure are illustrated in Fig. 3. n this method, instead of building predictor models simultaneously, an iterative and incremental algorithm is utilized. This process entails creating and incorporating simple basic structures (polynomial neurons) gradually. Through the combination of these basic structures, a sophisticated

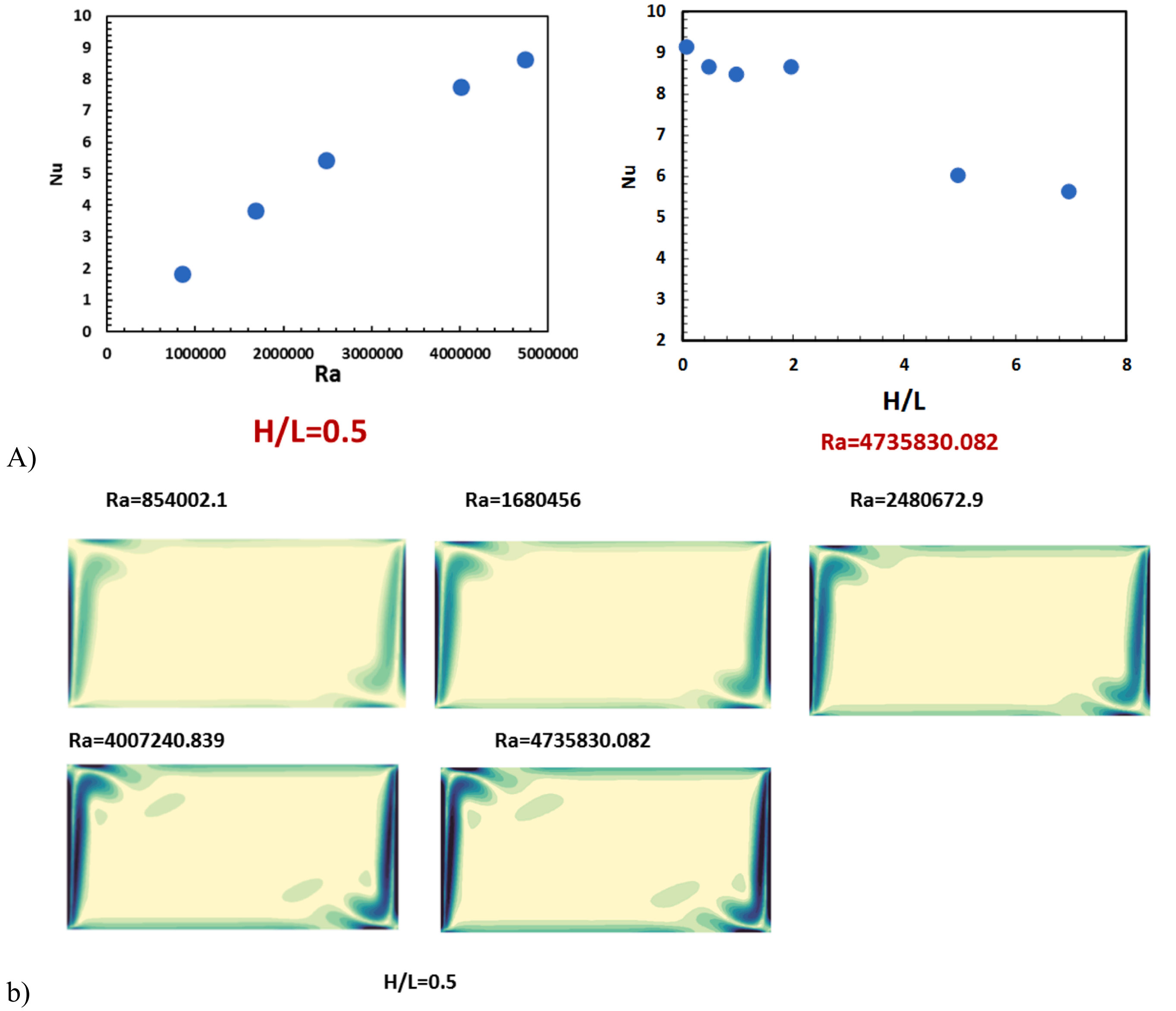

Fig. 4. The efficacy of H/L ratio, Ra on Nu and vorticity contour.

system with optimal performance is formed. One of the key algorithms for constructing the GMDH model, referred to as the polynomial NN, is the algorithm pioneered by Ivakhnenko. This algorithm relies on a quadratic polynomial model and a least squares error approach. The artificial neural network method based on GMDH is utilized to establish relationships from experimental data obtained from various experiments. The ANN and linear regression methods are merged to form polynomial NNs. In these networks (Fig. 3b), several polynomial expressions are treated as neurons in each layer of the network. In this study, to convert the experimental data obtained from various experiments into the relationship is based on the artificial neural network method based on GMDH. Artificial neural network and linear regression method are combined together and form polynomial neural networks. In these networks, a number of polynomial expressions are considered as neurons in each layer of the network. Considering the artificial neural network based on GMDH, the square of the differences between the predicted($\hat{y}_i$) and actual values(y_i) should be minimized and the coefficients $a_0, a_1, a_2, \cdots, a_4$ should be determined.

$$\sum_{i=1}^{M}(\hat{y}_i - y_i)^2 \underset{\rightarrow}{M}in. \tag{9}$$

$$\hat{y}_i = G(x_i, x_j) = a_0 + a_1x_i + a_2x_j + a_3x_ix_j + a_4x_i^2 + a_5x_j^2 \tag{10}$$

In order to assess the disparity between the outcomes of the GMDH-based NN, R^2 and RMSE have been employed. It is important to mention that the data is partitioned into two sets: training data and test data. The training data is used to calculate the coefficients of equation (10), whereas the evaluation of the GMDH-based NN is performed using the test data. It is important to highlight that the GMDH can accurately forecast output data within the range of trained input data only.

3. Discussion and results

In this study, the effect of *Ra* change, fluid type change, use of magnetic field, sinusoidal wall and mechanical vibrations on HT from the chamber has been examined.

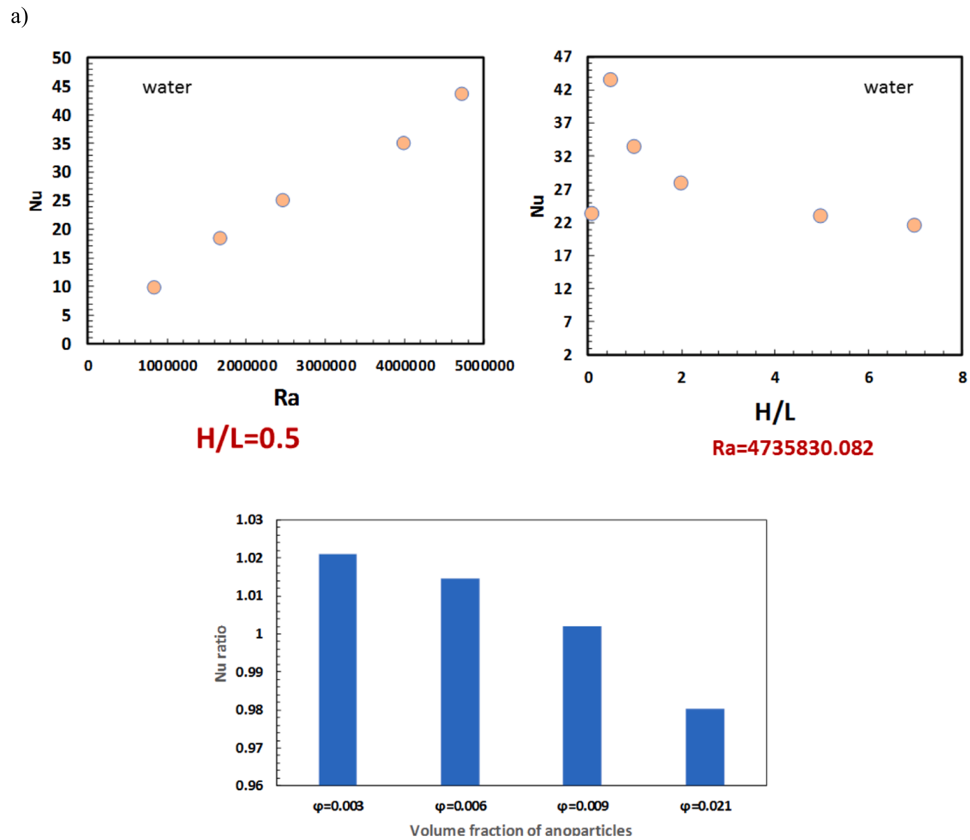

Fig. 5. The efficacy of H/L ratio, Ra on Nu for water and Nu ratio in terms of..φ

3.1. Effect of geometric parameters and flow on Nu

The effect of *Ra* on *Nu* in H/L=0.5 is checked and shown in Fig. 4a. The results show that *Nu* has increased with the increment of *Ra*. With the increment of the *Ra*, the ∇T and the temperature difference in the fluid increase. For this reason, the amount of buoyancy force increases and the role of convection mechanism in HT increases. Therefore, with the increment of the buoyancy force, the strength of the rotating current inside the chamber has increased and the vortex has been developed to the right and the center of the chamber, which is well presented in the contours. In fact, with the increment of the *Ra*, the convection mechanism will play a more effective role in the fluid compared to the thermal conduction. It is also observed that with the increment of H/L, the fluid volume in the chamber increases and at a constant *Ra*, the ability to overcome the buoyancy force over the viscous force decreases. Therefore, fluid movement and mixing of hot and cold fluid in the chamber is reduced and ultimately leads to a reduction in HT.

Also, when the agent fluid is water and nanofluid, the effect of *Ra* and H/L has been investigated and the results are shown in Fig. 4b and 5. In this case, the *Nu* has increased with the increment of the *Ra*. In the investigation of the H/L effect, it can be seen that with the rise of the H/L from 0.1 to 0.5, the value of the *Nu* augments until it attains a greatest value and then begins to decrease. The reason for this can be that with the increase in the length of the hot wall area, more fluid is located next to the wall, which is due to the condition of not sliding isothermally with the hot wall, which can help to mix and augment the average temperature of the fluid, and this mainly reduces The buoyancy force is similar to the viscous force and until H/L=0.5 this phenomenon reaches its maximum value (while the maximum *Nu* has been observed for air fluid at H/L=2) and after that the amount of hot fluid increases. Near the wall, it cannot overcome the weakening of the buoyancy force to the greater volume of the fluid and moving it in the chamber and reducing the convection of the fluid in the chamber, and it is observed that the *Nu* decreases. Compared to air fluid, water has a higher thermal conductivity coefficient and higher viscosity, and since the convection mechanism actually includes heat transfer through molecular diffusion and fluid mass movement, heat transfer is higher with water fluid. Furthermore, the impact of introducing Al_2O_3 NPs into H_2O and varying its volume fraction on *Nu* has been examined in Fig. 5. The properties of nanofluid are calculated based on the relationships and thermophysical characteristics presented in Fig. 1. The results show that with the intensification in φ, the ratio of *Nu* has decreased and at $\varphi = 0.003$, the *Nu* has improved compared to the state without nanoparticles, and this increase is about 2 %, and at $\varphi = 0.021$, the *Nu* has enhanced compared to the state without nanoparticles. In fact, the presence of NPs improves the k, and on the other hand, the ρ and μ of the NF augments compared to the base fluid. In smaller φ, mounting.

k and conductive HT can help to augment the mean temperature of the fluid and help the buoyancy force to overcome the viscous force, but with the increase of φ, the weakening efficacy of the viscous force on the flow convection in the chamber increases. The augment of the conduction mechanism is overcome and the *Nu* decreases.

3.2. Effect of altering the waveform of a heated surface on Nu

The study examined the impact of changes in the waveform of a heated wall on the Nu for air. The results are presented in Fig. 6. The influence of amplitude (A) and frequency (f) of oscillations on Nu was analyzed. Sinusoidal oscillations of the left wall were found to push the hot fluid towards the chamber's center, enhancing mixing with cold fluid due to disturbances created. Fluctuations in the heated wall intensified the inertia force, aiding buoyancy force in overcoming viscosity force and improving flow circulation. Flow fluctuations transformed transverse fluid movement into rotational motion, elevating average fluid temperature. On average, Nu increased by 196 % compared to no wall oscillation state. Nu changes were weakly

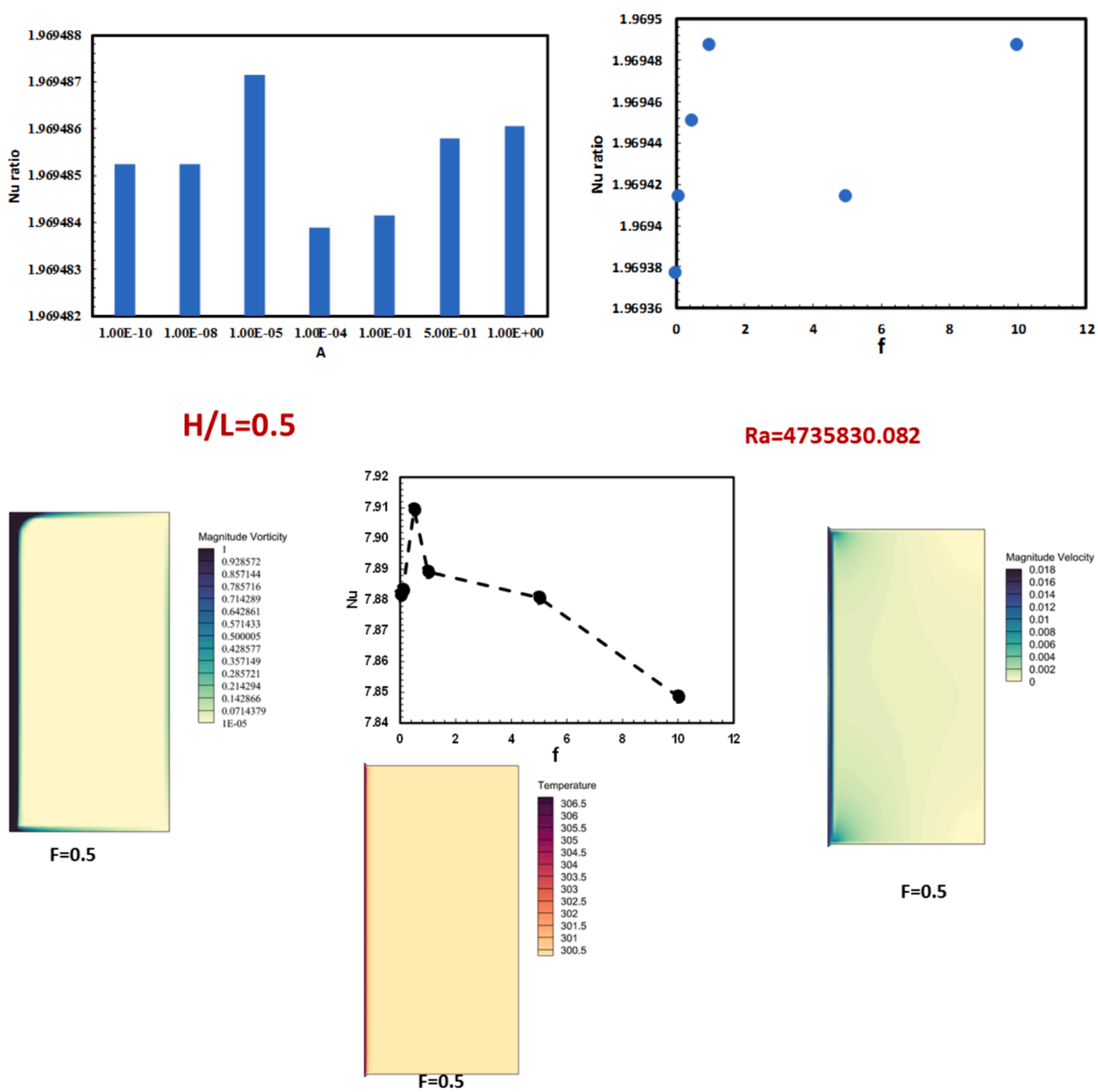

Fig. 6. The efficacy of *f* and *A* on *Nu* and vorticity, velocity and temperature contours.

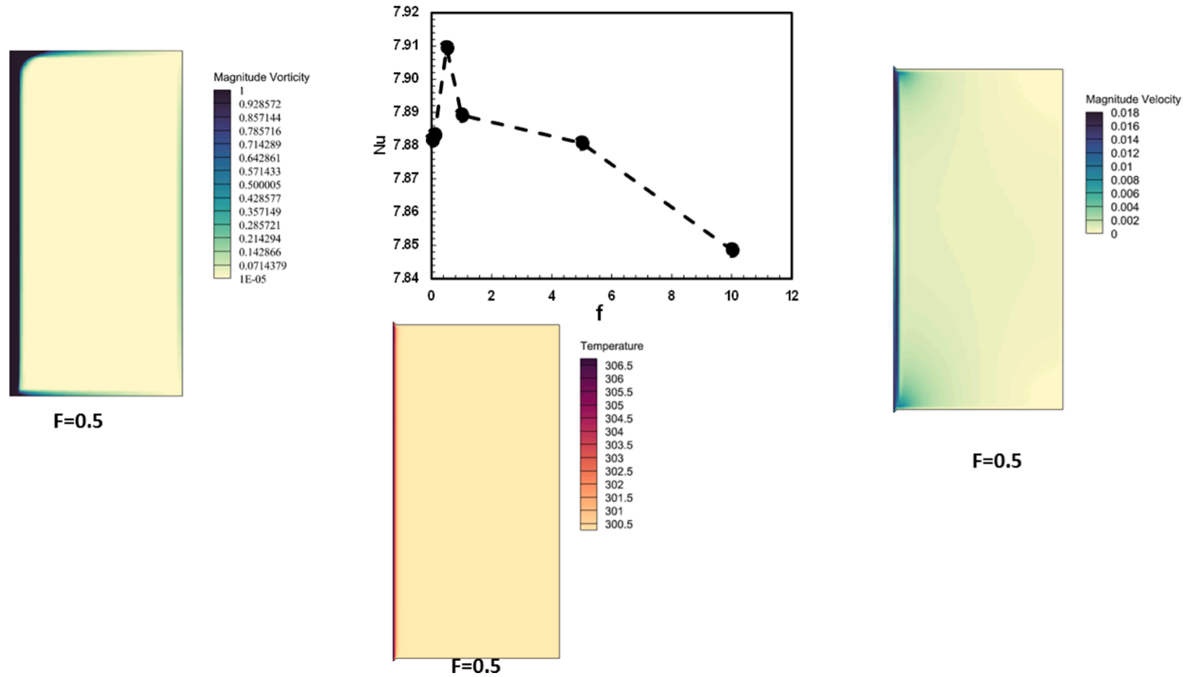

Fig. 6. (*continued*).

dependent on oscillation amplitude and frequency, with maximum Nu observed at $A = 10^{-5}$ and f = 5 Hz. The effects of Nu changes with Ra and aspect ratio (H/L) were also investigated. Nu amplified with Ra, particularly influenced by sinusoidal wall deformation at lower Ra values. As Ra augmented, buoyancy force strengthened, promoting natural convection expansion in the chamber. Higher Ra levels reduced the impact of hot wall fluctuations, with buoyancy force becoming dominant. Consequently, Nu increases slightly less with higher Ra, while more pronounced changes were observed at lower Ra values.

3.3. *Efficacy of transverse mechanical vibrations on Nu*

In the following, the impact of transverse mechanical vibrations on convection HT is examined, and the impact of ω and A of mechanical vibrations on the *Nu* is assessed in Fig. 7. With the escalation in amplitude and frequency of oscillations, the 's value has witnessed an increase compared to the state absent of vibration. It is evident that the mechanical vibrations induced within the fluid instigate the transverse motion of the fluid to transform into rotational motion, and the convection zones progressively expand as time elapses in the entire chamber (as illustrated in the velocity and temperature contours in Fig. 7). This action triggers the mixing of hot and cold fluids, leading to enhanced HT within the chamber. By augmenting the amplitude of vibrations from 0 to 0.01, 0.1, 0.5, 1, 10, and 100, respectively, an increase in the *Nu* is observed by 2.56 %, 19.23 %, 32.05 %, 41.03 %, 58.97 %, and 74.36 %, respectively, compared to the state without vibration. The elevation in the fluctuation range results in an escalation in the velocity and expansion of natural convection zones within the chamber, which magnifies with the upsurge in the range of force acting on the fluid. Subsequently, the mixing of hot and cold fluids improves, ultimately augmenting the *Nu*. By increasing ω from 0 to 0.1, 0.5, 1, 5, and 10, an increase in the *Nu* is observed by approximately 38.46 %, 54.49 %, 56.41 %, 60.26 %, and 75.64 %, respectively.

3.4. *Prediction of Nu using artificial intelligence*

In what follows, using the GMDH model, Nu is calculated based on Ra, H/L, f/A, and ω/A. There are about 45 data points based on the provided numerical solution. 85 % and 15 % of the data have been utilized for model training and test, respectively. In training data, the lowest and supreme values of each feature are included in the training data section so that the model error can be reduced. The GMDH-based NN is able to forecast output data with high accuracy only in the range of input data that has been trained, and it is only in this range that this network can be used. The results of the GMDH model prediction, error analysis, and model accuracy are well shown in Fig. 8. The outcomes clearly display that the GMDH model has been able to forecast *Nu* in this situation with high accuracy.

4. Conclusion

In the current examination, the numerical scrutiny of natural convection heat transfer (HT) in a rectangular chamber under the influence of the wall with sinusoidal deformation and mechanical vibrations using the finite volume method has been done. The consequence of dimension change, fluid type, sinusoidal change of hot wall and mechanical vibrations on the Nusselt number (*Nu*) in the chamber have been examined. The results are summarized below:

- As *Ra* rises, *Nu* increases, and with the intensification in the width-to-length ratio of the chamber, the HT first increases and then decreases. The value of the width-to-length ratio at which the *Nu* is extreme depends on the type of fluid, such as for air and water. It is obtained in the value of 2 and 0.5, respectively. The use of nanoparticles on HT can have a positive or negative effect, which depends on the nanoparticle volume fraction (NPVF). In low volume fractions, it can improve HT, and with an increment in NPVF, it can lead to a decrement in HT.
- The sinusoidal deformation of the warm wall is effective in expanding the HT and an increase of about 196 % in *Nu* was observed. The efficacy of frequency(f) and amplitude(A) of wall sinusoidal oscillations on *Nu* was investigated and the highest *Nu* was observed at A=10^{-5} and f = 5 Hz. In small *Ra*, the effect of sinusoidal fluctuations of the hot wall is more effective on improving HT
- The efficacy of the transverse vibrations of the chamber on the HT from the chamber was investigated and it was observed that there is an increase in the HT in about 2.56–75 % relative to the case without

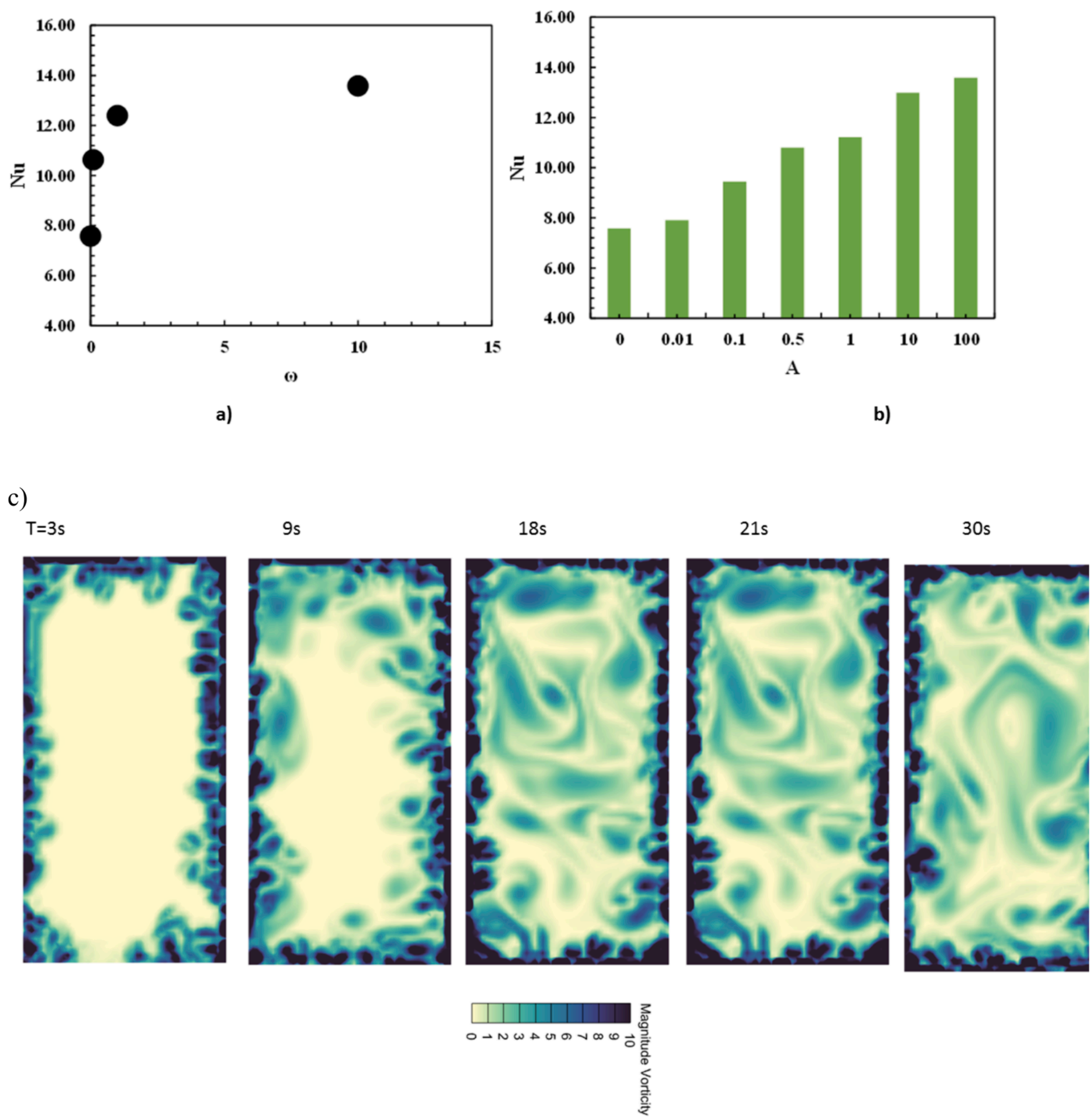

Fig. 7. Efficacy of a) frequency and b) amplitude of mechanical vibrations on Nu, c) Vorticity and d) temperature contour in several times.

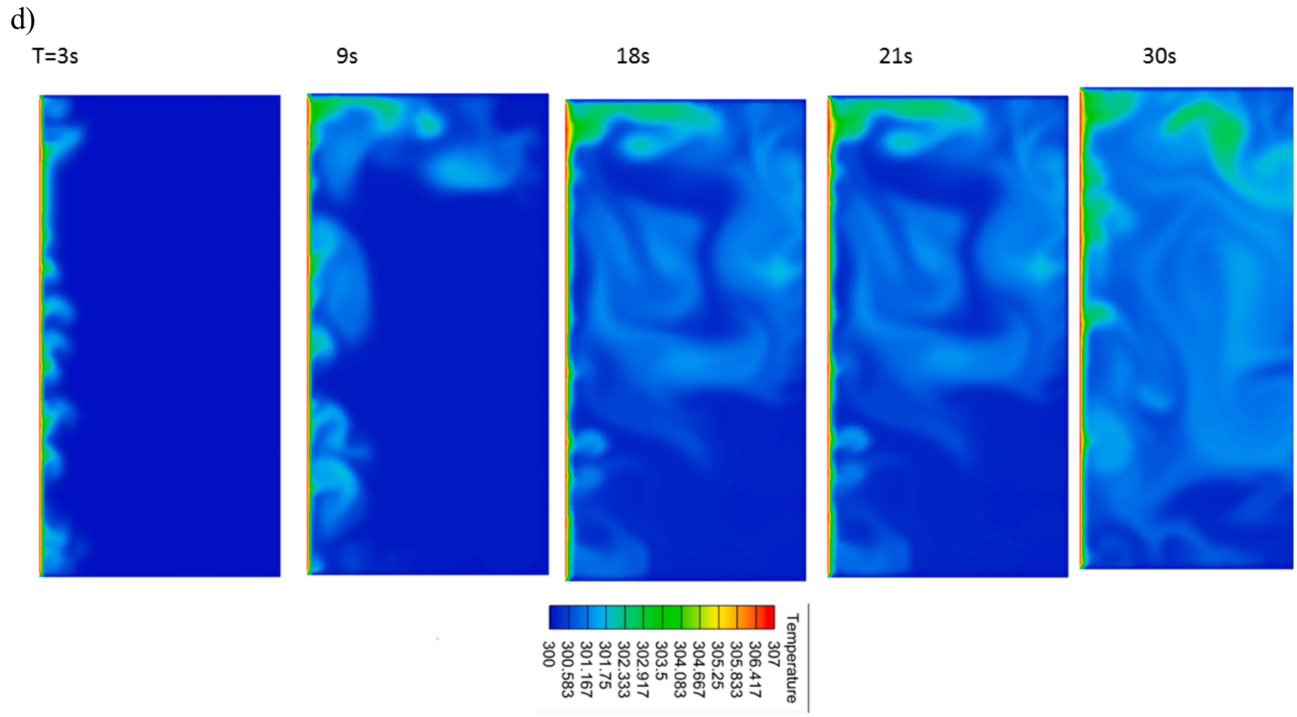

Fig. 7. (*continued*).

		R^2	RMSE
Train data	85%	0.9505	0.68472
Test data	15%	0.9606	0.67854
All data	100%	0.94809	0.69116

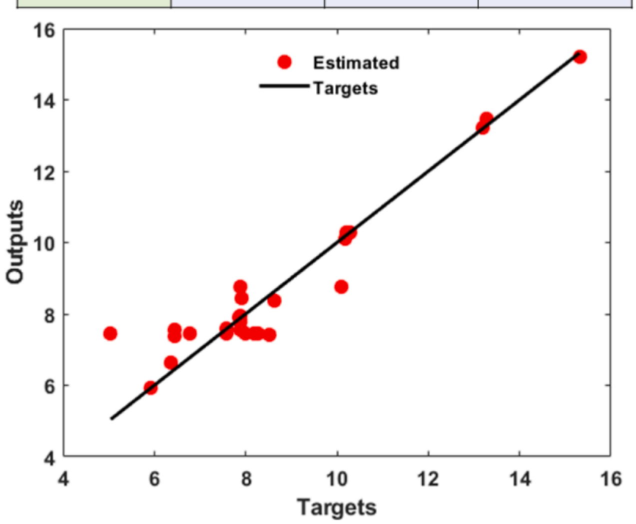

Fig. 8. Modeling results for..*Nu*

vibration. By increasing the amplitude and frequency of transverse vibrations, the HT in the chamber increases.

- Also, based on the available data and using the GMDH model, the *Nu* has been estimated and the said model has been able to approximate *Nu* very accurately.

CRediT authorship contribution statement

Somayeh Davoodabadi Farahani: Writing – review & editing, Writing – original draft, Visualization, Validation, Software, Resources, Project administration, Methodology, Investigation, Formal analysis, Data curation, Conceptualization. **As'ad Alizadeh:** Writing – review & editing, Writing – original draft, Visualization, Conceptualization. **Mohammed A. Tashkandi:** Conceptualization, Visualization, Writing – original draft, Writing – review & editing. **Lioua Kolsi:** Software, Visualization, Writing – review & editing. **Aliakbar Karimipour:** Conceptualization, Software, Visualization, Writing – review & editing.

Declaration of competing interest

The authors declare that they have no known competing financial interests or personal relationships that could have appeared to influence the work reported in this paper.

Acknowledgment

The authors extend their appreciation to the Deanship of Scientific Research at Northern Border University, Arar, KSA for funding this research work through the project number "NBU-FPEJ-2024-2028-05".

References

[1] Vakacharla BK, Rana BK. Free convection heat transfer from a spherical shaped open cavity. J Heat Transfer 2022;144(9):092601.
[2] Ali N, Nazeer M, Javed T. Finite element simulations of free convection flow inside a porous inclined cavity filled with micropolar fluid. J Porous Media 2021;24(2).
[3] Das Karmakar S, Dutta P, Chattopadhyay H. Free convection in a differentially heated square cavity filled with low-Prandtl-number materials: Numerical studies using transition shear stress transport model. Phys Fluids 2024;36(3).
[4] Nakamura H, Asako Y, Naitou T. Heat transfer by free convection between two parallel flat plates. Numer Heat Transf Part A Appl 1982;5(1):95–106.
[5] Salahi H, Sharif MA, Rasouli S. Laminar mixed convective heat transfer in a shallow inclined lid-driven cavity filled with nanofluid. J Therm Sci Eng Appl 2015;7(4):041016.
[6] Alsabery A, Sheremet M, Ghalambaz M, Chamkha A, Hashim I. Fluid-structure interaction in natural convection heat transfer in an oblique cavity with a flexible oscillating fin and partial heating. Appl Therm Eng 2018;145:80–97.

[7] Saleh H, Siri Z, Hashim I. Role of fluid-structure interaction in mixed convection from a circular cylinder in a square enclosure with double flexible oscillating fins. Int J Mech Sci 2019;161:105080.

[8] Kim B, Lee D, Ha M, Yoon H. A numerical study of natural convection in a square enclosure with a circular cylinder at different vertical locations. Int J Heat Mass Transf 2008;51(7–8):1888–906.

[9] Sourtiji E, Ganji D, Seyyedi S. Free convection heat transfer and fluid flow of Cu–water nanofluids inside a triangular–cylindrical annulus. Powder Technol 2015;277:1–10.

[10] Alqahtani AM, Sajadi SM, Al Hazmi SE, Alsenani TR, Alqurashi RS, El Bouz M. Entropy generation and mixed convection in an enclosure with five baffles exposed to a uniform magnetic field with volumetric radiation for the solar collectors via lattice Boltzmann method. Eng Anal Bound Elem 2023;150:285–97.

[11] Bouanani M, Benbrik A, Lemonnier D, Cherifi M, Soualmi R. Natural convection and volumetric radiation interactions in a concentric square annulus. J Thermophys Heat Transfer 2021;35(3):547–59.

[12] Biswas N, Mandal DK, Manna NK, Gorla RS, Chamkha AJ. Hybridized nanofluidic convection in umbrella-shaped porous thermal systems with identical heating and cooling surfaces. Int J Numer Meth Heat Fluid Flow 2023;33(9):3164–201.

[13] Mondal MK, Mandal DK, Biswas N, Manna NK, Al-Farhany K, Chamkha AJ. Enhanced magneto-convective heat transport in porous hybrid nanofluid systems with multi-frequency nonuniform heating. J Magn Magn Mater 2023;577:170794.

[14] Mandal DK, Biswas N, Manna NK, Gorla RSR, Chamkha AJ. Hybrid nanofluid magnetohydrodynamic mixed convection in a novel W-shaped porous system. Int J Numer Meth Heat Fluid Flow 2023;33(2):510–44.

[15] Mondal MK, Biswas N, Mandal DK, Manna NK, Chamkha AJ. Assessment of thermal performance of hybrid nanofluid flow in a tilted porous enclosure by imposing partial magnetic fields. Waves Random Complex Media 2022:1–34.

[16] Biswas N, Chatterjee D, Sarkar S, Manna NK. Magneto-nanofluidic thermal transport and irreversibility in semicircular systems with heated wavy bottom under constant fluid volume and cooling surface constraints. Int J Numer Meth Heat Fluid Flow 2024;34(2):1021–59.

[17] Chatterjee D, Biswas N, Manna NK, Mandal DK, Chamkha AJ. Magneto-nanofluid flow in cylinder-embedded discretely heated-cooled annular thermal systems: Conjugate heat transfer and thermodynamic irreversibility. J Magn Magn Mater 2023;569:170442.

[18] Marin M, Öchsner A, Bhatti MM. Some results in Moore-Gibson-Thompson thermoelasticity of dipolar bodies. ZAMM-Journal of Applied Mathematics and Mechanics/zeitschrift Für Angewandte Mathematik Und Mechanik 2020;100(12):e202000090.

[19] Marin M, Hobiny A, Abbas I. Finite element analysis of nonlinear bioheat model in skin tissue due to external thermal sources. Mathematics 2021;9(13):1459.

[20] Datta A, Biswas N, Manna NK, Mandal DK. Thermal management of nanofluid filled porous cavity utilized for solar heating system. J Inst Eng (India): Ser C 2022;103(2):207–21.

[21] Chakravarty A, Biswas N, Ghosh K, Manna NK, Mukhopadhyay A, Sen S. Impact of side injection on heat removal from truncated conical heat-generating porous bed: thermal non-equilibrium approach. J Therm Anal Calorim 2021;143:3741–60.

[22] Manolagas SC. Role of cytokines in bone resorption. Bone 1995;17(2):S63–7.

[23] Fu W-S, Shieh W-J. Transient thermal convection in an enclosure induced simultaneously by gravity and vibration. Int J Heat Mass Transf 1993;36(2):437–52.

[24] H. Kimoto, H. Ishida, Vibration effects on the average heat transfer characteristics of the natural convection field in a square enclosure, Heat Transfer—Asian Research: Co-sponsored by the Society of Chemical Engineers of Japan and the Heat Transfer Division of ASME, 29(7) (2000) 545-558.

[25] Florio L, Harnoy A. Use of a vibrating plate to enhance natural convection cooling of a discrete heat source in a vertical channel. Appl Therm Eng 2007;27(13):2276–93.

[26] Razi YP, Maliwan K, Charrier-Mojtabi MC, Mojtabi A. The Influence of Mechanical Vibrations on Buoyancy Induced Convection in Porous Media. In: Handbook of Porous Media. CRC Press; 2005. p. 339–90.

[27] Sarhan A, Karim M, Kadhim Z, Naser J. Experimental investigation on the effect of vertical vibration on thermal performances of rectangular flat plate. Exp Therm Fluid Sci 2019;101:231–40.

[28] Ji J, Zhang J, Gao R, Shi B, Li X, Li F, et al. Numerical Research on Vibration-Enhanced Heat Transfer of Elastic Scroll Tube Bundle. J Thermophys Heat Transfer 2022;36(1):61–8.

[29] Ji J, Deng X, Zhang J, Li F, Zhou R. Study on Vibration and Heat Transfer Performances of a Modified Elastic Tube Bundle Heat Exchanger. In: Journal of Physics: Conference Series. IOP Publishing; 2022. p. 012043.

[30] Rasangika AHDK, Nasif MS, Pao W, Al-Waked R. Numerical investigation of the effect of square and sinusoidal waves vibration parameters on heat sink forced convective heat transfer enhancement. Appl Sci 2022;12(10):4911.

[31] Farahani SD, Alizadeh Aa. Thermal efficiency of microchannel heat sink: Incorporating nano-enhanced phase change materials and porous foam gradient and artificial intelligence-based prediction. Alex Eng J 2023;82:1–15.

[32] Sepehrnia M, Davoodabadi Farahani S, Hamidi Arani A, Taghavi A, Golmohammadi H. Laboratory investigation of GO-SA-MWCNTs ternary hybrid nanoparticles efficacy on dynamic viscosity and wear properties of oil (5W30) and modeling based on machine learning. Sci Rep 2023;13(1):10537.

[33] Farahani SD, Farahani AD. Machine learning models for predicting the performance of solar-geothermal desalination in different meteorological conditions. Ain Shams Eng J 2024;15(3):102591.

[34] Hemmatian A, Kargarsharifabad H, Esfahlani AA, Rahbar N, Shoeibi S. Improving solar still performance with heat pipe/pulsating heat pipe evacuated tube solar collectors and PCM: An experimental and environmental analysis. Sol Energy 2024;269:112371.

[35] Nemati M, Farahani SD, Armaghani T. A LBM entropy calculation caused by hybrid nanofluid mixed convection under the effect of changing the kind of magnetic field and other active/passive methods. J Magn Magn Mater 2023;566:170277.

[36] Farahani SD, Farahani AD, Mamoei AJ, Yan W-M. Enhancement of phase change material melting using nanoparticles and magnetic field in the thermal energy storage system with strip fins. J Storage Mater 2023;57:106282.

[37] Hu R, Sun S, Liang J, Zhou Z, Yin Y. A review of studies on heat transfer in buildings with radiant cooling systems. Buildings 2023;13(8):1994.

[38] Wu Y, Luo M, Chen S, Zhou W, Yu Y, Zhou Z. Numerical simulation study of the effect of mechanical vibration on heat transfer in a six-fin latent heat thermal energy storage unit. Int J Heat Mass Transf 2023;207:123996.

[39] Liu W, Yang Z, Zhang B, Lv P. Experimental study on the effects of mechanical vibration on the heat transfer characteristics of tubular laminar flow. Int J Heat Mass Transf 2017;115:169–79.

[40] Farahani SD, Farahani AD, Öztop HF. Natural convection in a rectangular tall cavity in the presence of an oscillating and rotating cylinder. Colloids Surf A Physicochem Eng Asp 2022;647:129027.

[41] Farahani SD, Sheikhi R, Kisomi MS. Natural convection heat transfer in the annular space by using novel fins and water droplets injection. Braz J Chem Eng 2022;39(2):441–54.

[42] Catton I. Natural convection in enclosures. International Heat Transfer Conference Digital Library. Begel House Inc.; 1978.

[43] J. Arnold, I. Catton, D. Edwards, Experimental investigation of natural convection in inclined rectangular regions of differing aspect ratios, (1976).

[44] Markatos NC, Pericleous K. Laminar and turbulent natural convection in an enclosed cavity. Int J Heat Mass Transf 1984;27(5):755–72.

[45] Lari K, Baneshi M, Nassab SG, Komiya A, Maruyama S. Combined heat transfer of radiation and natural convection in a square cavity containing participating gases. Int J Heat Mass Transf 2011;54(23–24):5087–99.

[46] Ivakhnenko A, Ivakhnenko G. The review of problems solvable by algorithms of the group method of data handling [GMDH]. Pattern Recognition and Image Analysis C/c of Raspoznavaniye Obrazov i Analiz Izobrazhenii 1995;5:527–35.

[47] Anastasakis L, Mort N. The development of self-organization techniques in modelling: a review of the group method of data handling. GMDH: Research Report-University of Sheffield Department of Automatic Control and Systems Engineering; 2001.